Nanoparticle formulation for intra-articular treatment of osteoarthritic joints

Simou, Konstantina; Pan, Piaopiao; Li, Qingguo; Jones, Simon W.; Davis, Edward; Preece, Jon; Zhang, Zhenyu j.

Document Version
Publisher's PDF, also known as Version of record

[Link to publication on Research at Birmingham portal](#)

Nanoparticle formulation for intra-articular treatment of osteoarthritic joints

Konstantina Simou [a], Piaopiao Pan [b], Qingguo Li [b], Simon W. Jones [c], Edward Davis [d], Jon Preece [e], Zhenyu J. Zhang [a,*]

[a] *School of Chemical Engineering, University of Birmingham, Edgbaston, Birmingham B15 2TT, United Kingdom*
[b] *School of Pharmaceutical Sciences, Guangzhou University of Chinese Medicine, Guangzhou 510006, PR China*
[c] *MRC-Versus Arthritis Centre for Musculoskeletal Ageing Research, Institute of Inflammation and Ageing, University of Birmingham, Birmingham B15 2TT, United Kingdom*
[d] *The Royal Orthopaedic Hospital NHS Foundation Trust, Bristol Road South, Birmingham B31 2AP, United Kingdom*
[e] *School of Chemistry, University of Birmingham, Edgbaston, Birmingham B15 2TT, United Kingdom*

ARTICLE INFO

ABSTRACT

Based on a proven concept of using nanoparticles to lubricate an articulating interface, we developed a set of formulations to demonstrate the feasibility of using polymeric nanoparticles as physical intervention for early stage osteoarthritis (OA). The biocompatible polymeric nanoparticles (NPs), namely polymethylmethacrylate (PMMA), polycaprolactone (PCL), and polylactic acid (PLA) were accompanied with hyaluronic acid (HA) and surface actives, of which the lubrication effect was examined between a steel ball and a silicone elastomer substrate to replicate the bone-cartilage contact. All three types of polymer nanoparticles were found to reduce the overall Coefficient of Friction (CoF), with PLA NPs being the most effective - providing a reduction up to 24.3%, which suggests that soft (low Young's modulus) nanoparticles are the most efficient frictional additives. Based on the data acquired, it is likely that surface deposited NPs could smooth the solid substrates, hyaluronic acid ensures bulk viscosity, and the surfactant enhances formulation stability. We suggest that surface adsorbed nanoparticles are beneficial in providing interfacial lubrication, which offers insight on the development of early stage intervention strategies for OA.

1. Introduction

Over the course of osteoarthritis (OA), the mechanical properties of an articular cartilage (AC) deteriorate, and the synovial fluid (SF) loses its viscoelasticity [1]. Joint pain, stiffness, and eventually loss of mobility are associated with a poor joint lubrication [2]. For early stage OA, patients are recommended to follow a set of treatment with analgesics including oral and topical non-steroidal anti-inflammatory drugs (NSAIDs), or steroids [3], which might cause gastrointestinal and cardiovascular side effects [4,5]. Furthermore, these therapeutic approaches are not effective enough to hinder disease progression by mitigating tissue degeneration at the early stages of OA, which leaves joint replacement the only option in the end stage of OA [6].

As an alternative, intra-articular injection (IAI) has been introduced as a treatment for early OA [7], whereby therapeutic compounds are directly injected into a joint [8,9], which limits potential side effects [4,8,9]. In addition, IAI addresses the limited bioavailability of drugs as the result of oral administration [4,8,9]. However, current IAI formulations offer short-term pain relief (maximum six months) because the small drug molecules diffuse away from the joint via porous cartilage [8]. Furthermore, despite restoring the viscoelasticity of synovial fluid's (SF) via supplements (e.g. Hyaluronic acid (HA)), these are not able to counteract the increase of Coefficient of Friction (CoF) [10,11]. The increased viscosity, compensated by the injection of IAI formulation, could not moderate the increase of the CoF in the boundary regime [10], which represents low-velocity movements such as walking.

Surface active polymer, either synthetic or bio-based, has been used to improve the lubrication of synovial joints by chemically grafting or physically adsorbing on the AC surface [12]. In parallel, a range of nanoparticles (NPs) have been reported to reduce CoF at an articulating interface, proposing mechanisms such as ball bearing effect, surface polishing effect [13–18]. Hybrid NPs, where polymer chains grafted on

NPs, have shown significant CoF reduction [13–16], which is attributed to the formation of a hydration layer on the NPs [19]. Polymeric NPs proved to deliver promising potential for minimising joint damage and inflammation in many types of arthritis [8,20,21], and their capability to improve joint lubrication has already been demonstrated in a few studies [12].

NPs made of Polymethylmethacrylate (PMMA), Polycaprolactone (PCL), and Polylactic acid (PLA) were selected in this study because they are biocompatible, whereas PCL and PLA are also biodegradable, and therefore, do not accumulate in the human body [22,23]. Their usage in IAI formulation is feasible since they have already been approved for biomedical applications, for example, the US Food and Drug Administration (FDA) has authorised the use of PMMA in bone cement implants [24]. FDA has also approved PLA as a filler for the repair of meniscus and bone implants and as a material for artificial scaffolds, sutures and screws [22,25]. PCL has been certified as FDA approved for use in various medical applications, including sutures and scaffolds for regeneration of AC [26,27]. The mechanical and physical properties of the PMMA, PCL, and PLA NPs are summarised in Table 1.

In the present work, we hypothesized that polymeric NPs could improve the lubrication characteristics of the synovial joint, specifically at the early stage of OA. Biocompatible NPs and surfactants were mixed with HA to prepare a series of formulations, of which the tribological properties were quantified between two surfaces in contact to simulate synovial joints. The aim is to demonstrate the feasibility of complex polymeric NPs based formulations in lubricating physiologically relevant contact as the first step for treatment of early stage OA. We characterised the hydrodynamic size and stability of several polymeric NPs in the presence of HA and synthetic surface actives, evaluated their effect of the rheological profile of the bulk fluid, and subsequently quantitatively investigate the tribological properties of the developed formulations.

2. Materials and Methods

2.1. Preparation of Polymeric Nanoparticles

Polymer (50 mg), including PMMA (Shanghai Macklin Biochemical Co., Ltd., China), PCL (Shanghai Yuanye Bio-Technology Co., Ltd., China), and PLA (Shandong Academy of Pharmaceutical Sciences, China), was dissolved in dichloromethane (10 mL) to form a homogeneous organic phase. The organic phase was added into 40 mL 2% Polyvinyl Alcohol (PVA) solution (Shanghai Aladdin Bio-Chem Technology Co., Ltd., China), followed by homogenization (ATS Engineering Inc., Shanghai, China) at 800 bar for 3 cycles. The suspension was added into 150 mL 2% PVA solution, after a continuous stirring for 4 h to evaporate dichloromethane, the suspension was subsequently centrifuged at 13,000 rpm for 25 min at 4 °C. The pellet was resuspended in de-ionised water by sonication for 60 s and centrifuge again, repeating the wash steps twice. After washes, the pellet was resuspended in de-ionised water by sonication and maintained at −80 °C for 2 h before being lyophilized for 37 h.

2.2. Preparation of Nanoparticle Formulations

The prepared NPs was added to a Phosphate Buffered Saline (PBS) solution (Fisher Scientific, UK) to form 0.01, 0.1, 0.5, and 1% w/v suspension, alongside 0.1% w/v HA (Bloomage Freda Biopharm Co., Ltd., China) and 0.5% w/v SDS (Fisher Scientific, UK), followed by magnetic stirring until the NPs were dispersed, and subsequently three hours of ultrasonic agitation.

2.3. Characterisation of Polymeric Nanoparticles

Hydrodynamic diameter and zeta potential (ZP) measurements were performed by a light scattering setup (Nano ZS, Malvern Panalytical, UK) equipped with a He—Ne laser (633 nm) at 25 °C. The refractive indices used to calculate PMMA, PCL, and PLA NPs are 1.49 [31], 1.50 [43], and 1.47 [44], respectively. The aqueous medium in which the NPs were diluted was High Performance Liquid Chromatography (HPLC) water (Fisher Scientific, UK), of which the refractive index is 1.33 and viscosity is 0.8872 cP. The size of the NPs formulations was presented as Z-average and corresponding polydispersity index (PDI). The average values were calculated as the mean average of three repeats.

2.4. Surface Morphology

Surface morphology of the SE discs was established using an Atomic Force Microscope (Multimode AFM, Bruker Ltd., UK) with an Intermittent Contact mode in ambient. Silicon cantilevers (Bruker Ltd., UK) with a spring constant of 42 N m^{-1} and resonance frequency of 320 kHz were used. An opensource software, Gwyddion, was used for image analysis.

2.5. Viscosity Measurements of Nanoparticle Formulations

Steady-state flow tests of the nanoparticle suspensions were conducted on a rheometer (HR-1 Discovery Hybrid Rheometer, TA Instruments, USA). A standard double concentric cylinder made of aluminium with a gap of 500 μm (TA Instruments, USA) was used as the measurement geometry. Viscosity of the samples was evaluated between shear rates 2–100 s^{-1} at a temperature of 37 °C. All samples were tested in triplicates.

2.6. Tribological Measurements of Nanoparticle Formulations

The tribological characteristics of the NP formulations were evaluated quantitatively using a Mini-Traction Machine (MTM2, PCS Instruments, UK) between a stainless steel ball of 19.05 mm diameter (PCS Instruments, UK) and a silicone elastomer (SE) disc of 46 mm diameter (Samco Silicone Products, UK). Measurements were conducted under a sliding velocity ranging 1–100 mm s^{-1} at 37 °C to simulate the movement of synovial joint. Conditions of pure sliding were applied (Slide-Roll-Ratio (SRR) = 200%). A new SE substrate was used for each measurement, whereas steel balls and the measurement chamber were cleaned thoroughly between each experiment.

The combination of substrates was selected to simulate the natural bone-cartilage contact. A stainless-steel ball was used to replicate bone due to its comparable stiffness and the SE disc for soft and rough AC.

Table 1
Literature reported values concerning the mechanical and physical properties of PMMA, PCL, and PLA NPs.

Nanoparticles	Young's modulus (GPa)	Water contact angle (°)	Density (Kg m^{-3})	Hardness (Shore D)	References
PMMA	2.03–3.01	77 ± 5	1190	96	[28–32]
PCL	0.33–0.38	80 ± 7	1145	55	[33–37]
PLA	1.28–7.00	79 ± 2	1252	76 ± 0.5	[38–42]

Table 2
Mechanical and morphological properties of specimen and real joint contacts.

Contact surfaces	Young's modulus (GPa)	Surface roughness (nm)	Poisson ratio (−)	References
AC	2.6–5.6 × 10^{-3}	72–114	0.40	[46–50]
Bone	3.3–15.3	–	0.30	[51,52]
SE disc	6.9 × 10^{-3}	94 ± 21	0.50	[53]
Steel ball	207	10.0	0.29	[53,54]

Their physical properties are presented in Table 2. Friction measurements were carried out under a constant contact pressure of 0.15 MPa, of which the corresponding contact area was 4.71×10^{-5} m^2, based on the Hertz model [45], sliding velocity between 1 and 100 mm s^{-1}, and at 37 °C.

2.7. Statistical Analysis

The friction results acquired by MTM were analysed using a Machine Learning Analysis (MLA) tool developed specifically for this study. It uses a linear, support vector regression, and random forest regression algorithms. To determine the quality and, therefore, the reliability of each model, the coefficient of determination (R^2), the mean absolute error, and the root mean squared error of each were displayed by the MLA tool. The closer the R^2 score is to 1, the closer the predictive data were to the actual data. Correlation coefficients (CC) were generated to identify the statistical importance of each parameter and the correlations between them. The greater the CC, the more significant its impact. A positive coefficient denotes a positive correlation and vice versa.

3. Results and Discussion

3.1. Characterisation of the Nanoparticle Formulations

Light scattering measurements were carried out to characterise the size, stability, and zeta potential of nanoparticles dispersed in the suspension, with or without the presence of SDS and HA. Our results suggest that the diameter of the pristine NPs was 200 ± 2 nm for PMMA, 225 ± 1 nm for PLA, and 244 ± 1 nm for PCL (Fig. 1a), and their corresponding zeta potential is nearly zero (Fig. 1c).

Representative surface active, a synthetic surfactant, SDS (0.5% w/v), was added to stabilise the NPs [55], which is evidenced by the approximately consistent averaged size for PMMA and PLA NPs, but not PCL (Fig. 1a). Addition of SDS did not have a significant impact on the PDI values, for all three NPs. We found that the surface adsorbed SDS was able to change the zeta potential of NPs to from approximately zero to nearly −40 mV for all three types of samples studied (Fig. 1c).

In another set of NPs formulations, HA was added to modulate their rheological profile. As reported in the literature [56], HA concentration is between 0.1 and 0.4% in healthy SF, although it decreases significantly as OA progresses. Four HA concentrations, 0.01, 0.05, 0.1, and 0.22%, were evaluated initially in PBS solution consisting of 0.5% NPs (PLA) and 0.5% SDS. The highest HA concentration examined (0.22%) represents the median SF concentration in healthy human knee joints [56]. HA concentration of 0.01% was not considered further because it was far less than the physiological concentration of HA in healthy SFs [56], although it provided a satisfactory reduction in CoF ($19.9 \pm 1.3\%$). Finally, the concentration of 0.1% HA was chosen because it resulted in the lowest average CoF (0.08) and had a satisfactory CoF reduction rate ($12.5 \pm 0.9\%$). It is worth noting that HA alone could lead NPs to aggregate (increased size) (Fig. 1a), evidenced by an increased PDI for all types of NPs (Fig. 1b). It is probable that NPs interact with the hydrophobic domains of HA and form NPs-HA complex due to the attractive depletion effect [57] – the size of the NPs aggregates was approximately two times greater than their initial size (Fig. 1a). This phenomena highlights the complexity of having multiple components in the formulation in delivering interfacial lubrication, and the potential challenge of introducing polymeric NPs into natural synovial fluid that contains HA, lubricin, albumin, phospholipids, and enzymes. A fundamental understanding required to advance the IAI technology is to determine the dominating tribological mechanisms when NPs, or artificial particulates of controlled geometry and properties, are present at the cartilage, alongside with the other biomolecules aforementioned.

The synergistic action of HA and SDS resulted in a stable formulation. Zeta potential of the final formulation was less than −25 mV for all three types NPs studied (Fig. 1c), confirming a satisfactory degree of stability.
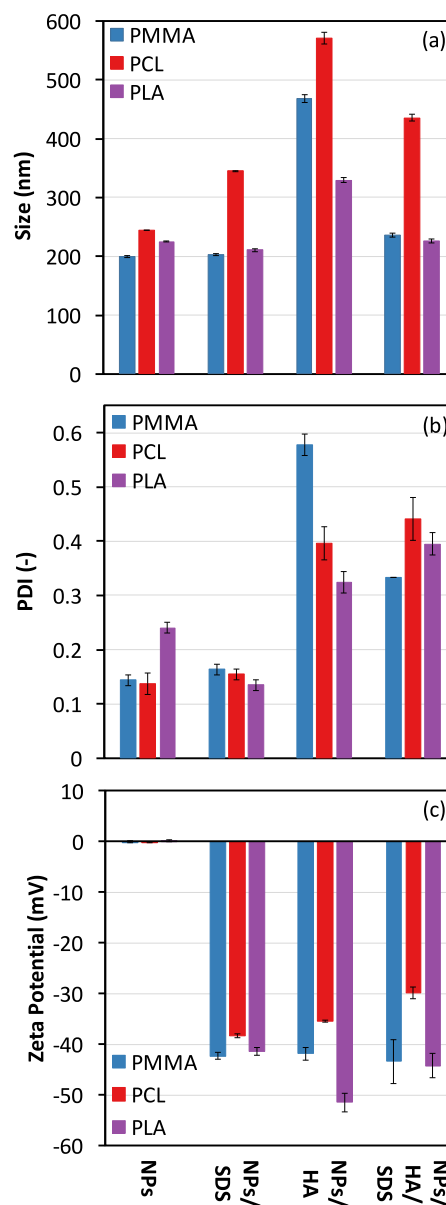

Fig. 1. (a) Hydrodynamic diameter, (b) PDI, and (c) zeta potential of PMMA, PCL, and PLA NPs (0.5% *w/v*) in water, SDS (0.5% w/v), HA (0.01% w/v), and HA (0.01% w/v)/SDS (0.05% w/v). The error bars represent the standard error from three repetitions.

When SDS and HA were added to the same NP formulation, SDS could adsorb on NP surface first because it diffuses faster than HA [58]. It is also possible that SDS formed complexes with HA in the bulk solution by hydrophobic interaction [59]. The PCL/HA/SDS formulation was not as stable as the other suspensions: its averaged size and PDI remained high (Fig. 1a and Fig. 1b) even in the presence of the SDS. In that case, the attractive depletion forces between the NPs might be too strong for SDS to keep them separated.

3.2. Effect of Nanoparticles on the Bulk Viscosity

Fig. 2 shows that all NP solutions, including the benchmark (PBS buffer), behaved as a Newtonian fluid. Their viscosity profiles were fitted with the Power-law model [60], of which the Power-law indices (n) were found above 0.97 (Table 3), confirming their Newtonian nature. This is consistent with literature whereby viscosity of polymer NPs
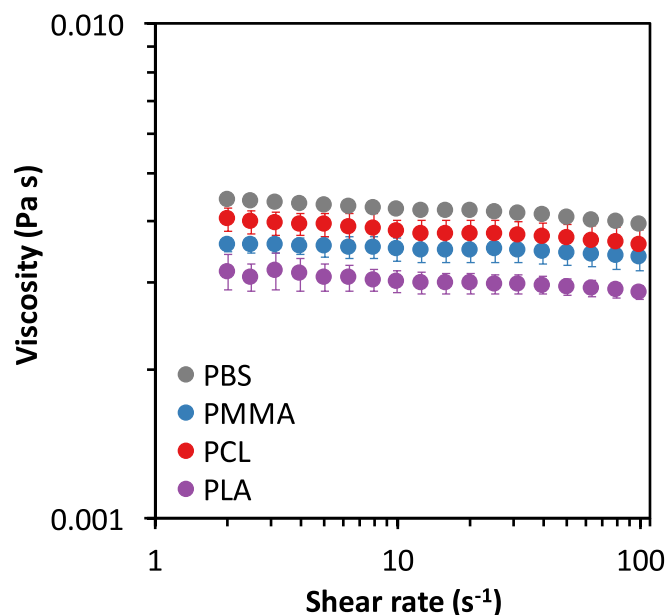
Fig. 2. Viscosity profile of PMMA, PCL, and PLA NPs formulations at 37 °C. The formulations were consisted of NPs (0.5%), HA (0.1%), and SDS (0.5%) in PBS. Error bars represent standard error from three repetitions of the same sample.

Table 3
Viscosity (η), consistency (m), Power-law index (n), and coefficient of determination (R^2) of PMMA, PCL, and PLA NPs formulations.

Formulations	η (mPa s)	m (mPa s)	n (−)	R^2 (−)
PBS	4.19 ± 0.03	4.50	0.97	0.97
PMMA	3.50 ± 0.01	3.60	0.99	0.92
PCL	3.80 ± 0.03	4.10	0.97	0.98
PLA	3.01 ± 0.20	3.20	0.98	0.93

suspension at low concentrations and low shear rates were found to follow Newtonian behaviour [61–63]. The NP formulations were semi-dilute (volume fraction: 0.004), which, based on the literature, are Newtonian [64]. Viscosity level of the formulations is dominated by HA [65]: although HA could increase the viscosity of pure PBS by 522%, shear-thinning behaviour of HA does not affect these formulations because the continuous phase (PBS buffer) dominates the rheological behaviour of HA solutions [66] at such low concentrations (0.1%) and low shear rates (2–100 s^{-1}).

It was found that all NPs/HA/SDS formulations present a viscosity less than the benchmark, PBS buffer (Fig. 2). Such reduction in the bulk viscosity is attributed to the presence of SDS because we observed that 0.5% SDS was able to reduce the viscosity of a 0.1% HA solution up to 7.5%. It is very probable that the SDS interacted with HA by hydrophobic interaction [59] and form molecular complex, which alters the viscosity profile of the solution [59]. Additionally, such hydrophobic interactions between surfactants and polymers result in conformational rearrangement and hydrodynamic radius of the HA chains. Another possible explanation for the reduced viscosity observed could be attributed to the dispersion methods (magnetic stirring, sonication) used to reduce the PDI, which inevitably increased the temperature of the samples and could have decreased the viscosity [67].

The viscosity of the different NP suspensions were slightly different, following the order of PCL > PMMA > PLA, which could be explained by the different tendencies of the NPs to aggregate. Aggregation of NPs could increase the active volume fraction of NPs in a suspension and form compact structures that are more resistant to flow than individual NPs, increasing the viscosity consequently [64,68,69]. There appears to

be a correlation between the particle size of the NPs in the final formulation (Fig. 1a) and the corresponding viscosity (Fig. 2): PCL NPs presented the largest average particle size of 436 ± 6 nm resulted in a formulation with the highest viscosity, whilst PLA NPs were of the smallest average particle size of 227 ± 3 nm, resulting in a formulation with the lowest viscosity. However, we would like to highlight that the differences in viscosity are at the magnitude of mPa and are considered insignificant.

### 3.3. Effect of Nanoparticle Formulations on the Tribological Characteristics

Fig. 3 shows the tribological characteristics of the PMMA NPs formulations developed as a function of sliding velocity and formulation composition. The CoF of the stainless steel vs SE substrate decreased for all tested velocities up to 28% with the addition of 0.5% SDS in PBS (Fig. 3a), which is likely because SDS could adsorb at the solid-liquid interface and act as lubricant additive [70]. Introducing PMMA NPs in the formulation was able to further decrease the CoF: for example, 0.5% PMMA NPs + 0.5% SDS reduced the CoF up to 34% (Fig. 3), which is attributed to the presence of NPs at the articulating interface. Based on the mechanisms proposed in the literature, we speculate that PMMA NPs were able to deposit on the SE surface, accumulate in the 'valley' region, render the elastomer substrate to become smoother, which reduces the overall CoF observed at the macroscopic scale [70].

Having HA alone in PBS buffer could reduce the CoF up to 28%, comparing to the benchmark (Fig. 3b), which could be attributed to HA's capability to increase viscosity in both bulk and the contact area [65]. It is worth noting that adding PMMA NPs to a HA formulation did not decrease the CoF in the sliding velocity range surveyed (Fig. 3b). This could be a consequence of NPs aggregation (Fig. 1), which alters the ability of PMMA NPs to deposit on the elastomer surface.

SDS and HA in PBS acted synergistically and achieved a higher reduction than each component separately (35% versus 28%), as shown in Fig. 3c. The significant reduction in CoF is linked to the adsorption of the SDS on the SE surface, and the increased viscosity provided by the HA. Adding 0.5% PMMA NPs in the HA/SDS/PBS solution provided the greatest CoF reduction of 41% (Fig. 3c). It is worth highlighting that the PMMA NPs formulation was more effective in the low sliding velocity region (up to 8 mm s^{-1}) than in the high velocities, likely because the contact mechanics is shifted from boundary to mixed regime, and the contribution of surface characteristics is less important. We would like to highlight that the materials properties of stainless steel and SE substrate are distinctively different to cartilage and bone in terms of surface chemistry, porosity, surface energy etc. Further in-vitro testing with cartilage and bone samples would be beneficial to test the observation reported.

3.4. Surface Morphological Characteristics of SE Substrate

To evaluate the hypothesis that the NPs were able to deposit on the elastomer surface, and consequently facilitate a significantly reduced macroscopic friction, surface morphological characteristics of SE were acquired using atomic force microscopy. At nanoscale, the elastomer used has a rough surface (R_a: 94 ± 21 nm), as shown in Fig. 4a – it is of the same order of magnitude to the size of the NPs used. Some spherical features could be observed on the SE surface after a friction test using SDS (0.5%) only in PBS (Fig. 4b), which confirms that SDS could adsorb on the elastomer surface, and reduce the interfacial friction. The presence of deposited NPs were observed explicitly on the SE surface after it was used in a friction test with 0.5% PLA NPs dispersed in PBS (Fig. 4c). Based on the AFM image, surface coverage of PLA NPs on the SE substrate is $15.4 \pm 2.6\%$, confirming the polishing effect mechanism [70]. The SE sample presented in Fig. 4d was treated with the complete formulation, in which individual NPs adsorbed on the surface can be seen.
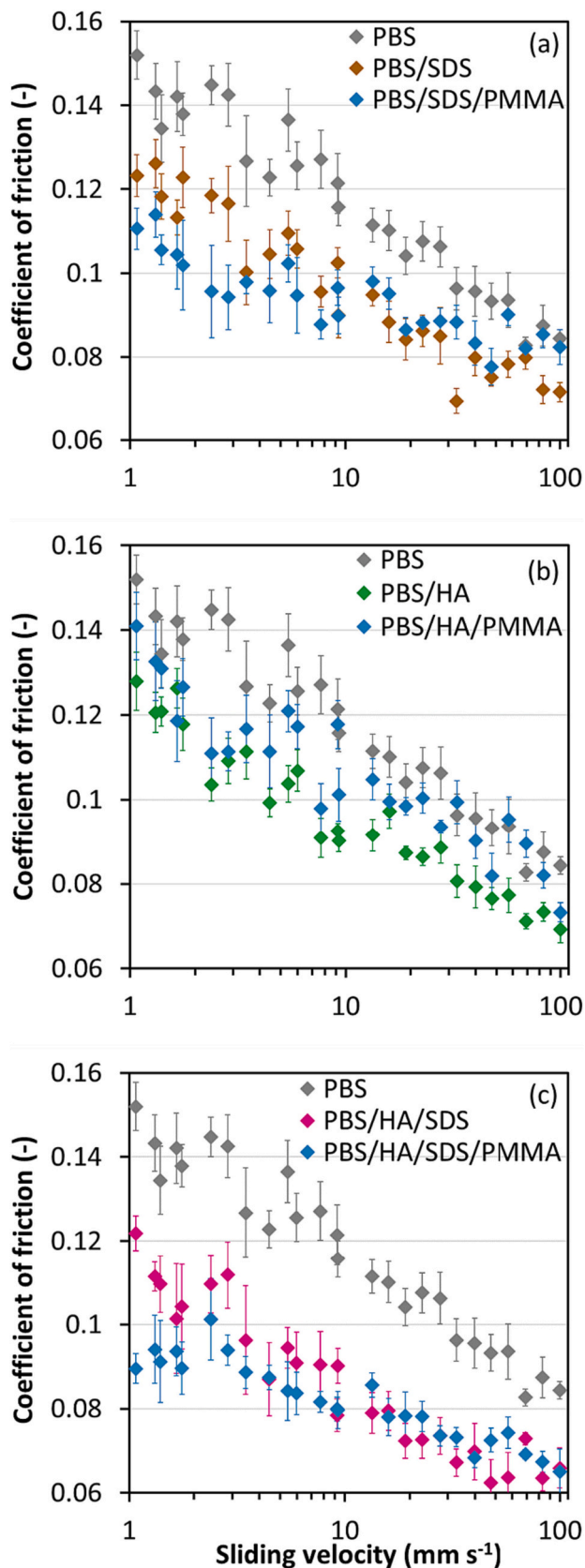
Fig. 3. Effect of (a) SDS, (b) HA, (c) SDS and HA on the coefficient of friction between a steel ball and a SE substrate as a function of sliding velocity. The concentration of NPs and SDS was 0.5% *w/v*, whereas the concentration of HA 0.1% w/v.

In summary, the images of the elastomer samples used after our tribological testing (Fig. 4) confirm the contribution of the formulation components to its lubrication performance. The SDS adsorbed on the surface of SE and minimised the contact of the opposing surfaces, the NPs turned the surface smoother by filling its valleys. Lastly, no wear track was observed on the surface of the used SE, which supports the proposed lubrication mechanism of the formulations developed.

3.5. Effect of Nanoparticle Concentration on the Coefficient of Friction

Friction tests with three NPconcentrations of 0.1%, 0.5%, and 1% were carried out under the same experimental condition, whilst the concentrations of HA (0.1%) and SDS (0.5%) were kept constant in the PBS buffer. All three NPs, PMMA, PCL, and PLA, presented a similar tribological characteristics. For data clarity, the effect of PLA NP concentration on the macroscopic CoF is presented below in Fig. 5a. It can be seen that the formulation with 0.1% PLA NPs resulted in some reduction with CoF (8.5%), and showed a similar tribological behaviour to the benchmark (PBS buffer). Both PBS and the 0.1% NPs formulation exhibited a steep reduction in the low sliding velocity region (up to approximately 20 mm s^{-1}), which is an indication of mixed lubrication regime. As the NP concentration increased to 0.5% and 1%, there was a significant decrease with the CoF by 22.5% and 26.6%, respectively.

It should be noted that the formulation with high NP concentrations (0.5% and 1%) demonstrated a distinctively different tribological profile to that of low NP concentration: the CoF reached minimal from the outset, and remain at such low magnitude throughout the sliding velocities surveyed. This provides an indisputable evidence that the presence of NPs at the articulating interface is the primary reason for the lubrication observed. It is very probable that a concentration of 0.5% NPs was sufficient to fill the 'valleys' on the SE surface and lubricate the interface, whereby the decreasing CoF as a function of an increasing sliding velocity no longer presents. As the concentration was increased to 1% NPs, there could be some excessive amount of NPs on the surface, as described in Fig. 5b, of which the effect on lubrication was not noticeable. The drastic change of the tribological profile from 0.1% to 0.5% PLA NPs solutions confirms that adequate amount of NPs deposited at the articulating interface is crucial for a successful NP based IAI formulation, which implies that the attractive interaction between the nanoparticles and the substrates in contact could be an important design factor. Material properties in relation to the NPs used, in combination of those of the solid materials involved in a synovial joints, ought to be considered carefully in the future design of IAI formulation.

3.6. Effect of Nanoparticle Type on the Coefficient of Friction

Upon evaluating the effect of NP concentration on the overall lubrication, an optimum composition in terms of the CoF reduction performance was established as 0.5% NPs, 0.1% HA, and 0.5% SDS in PBS buffer. Formulations with PMMA, PCL, and PLA NPs were assessed by using the friction measurements between a steel ball and a SE substrate under the same experimental conditions. The limitation of such measurement configuration has been discussed in Sections 3.1 & 3.3. Fig. 6 presents the tribological characteristics of the model IAI formulations based on PMMA, PCL, and PLA NPs as a function of Hersey number.

It was found that all NP formulations were able to offer interfacial lubrication (reducing the CoF), confirming that the NPs presented at the entrainment area play a crucial role. However, at high Hersey number (above $6.4–8.9 \times 10^{-9}$, corresponding to a sliding velocity of 8 mm s^{-1}), the CoF of PMMA and PCL formulations was of the same levels with PBS (Fig. 6), probably because NPs were dislodged from the surface due to the high sliding velocity [71]. Based on the Stribeck curves generated, it is suggested that all NPs based formulations were in the mixed lubrication regime because their CoF was decreasing with an increasing Hersey number (Fig. 6), despite that the magnitude and rate of reduction
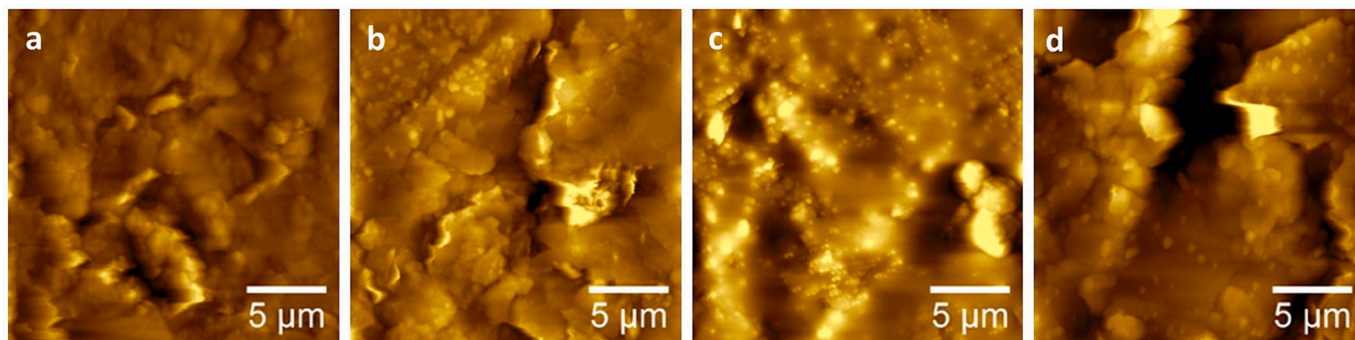
**Fig. 4.** AFM images of SE samples that are (a) clean, (b) used with SDS (c) used with PLA NPs, and (d) used with PLA NPs/HA/SDS. The concentration of NPs and SDS was 0.5%, whereas the concentration of HA 0.1%. All formulations were based on PBS. The size of the images is 400 μm^2.
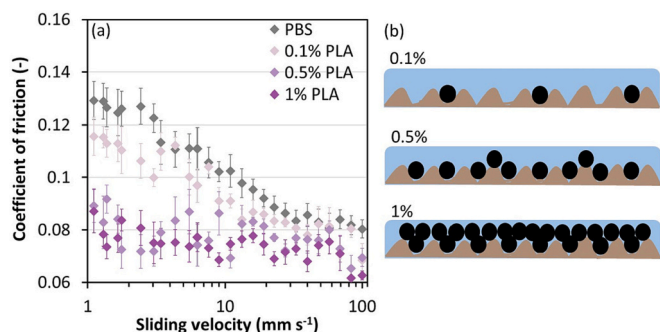
Fig. 5. (a) Effect of NPs concentration (0.1%, 0.5%, 1%) on the coefficient of friction developed between a steel ball and a SE substrate. (b) Schematic representation of the suggested lubrication mechanism. The formulations were consisted of PLA NPs/HA (0.1%)/ SDS (0.5%) in PBS.
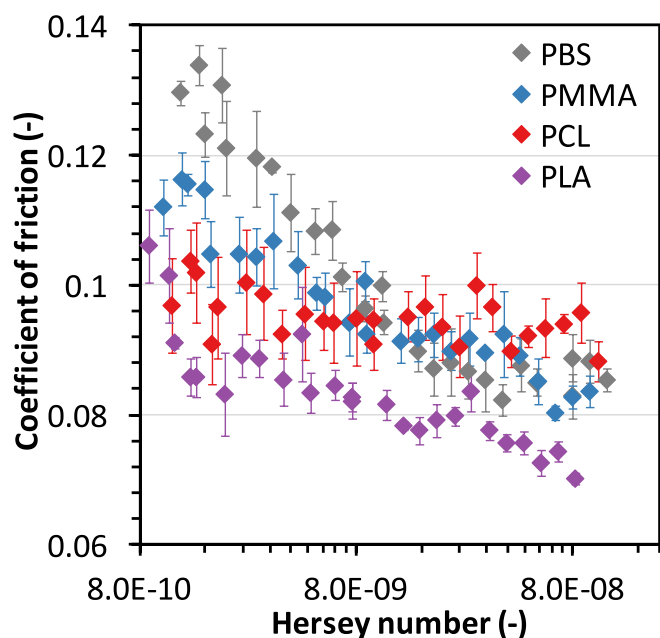
Fig. 6. Coefficient of friction of PMMA, PCL, and PLA nanoparticle formulations between a steel ball and a SE substrate as a function of Hersey number. Formulations were consisted of NPs (0.5%)/HA (0.1%) /SDS (0.5%) in PBS. Error bars represent the standard error of five repetitions of the same sample.
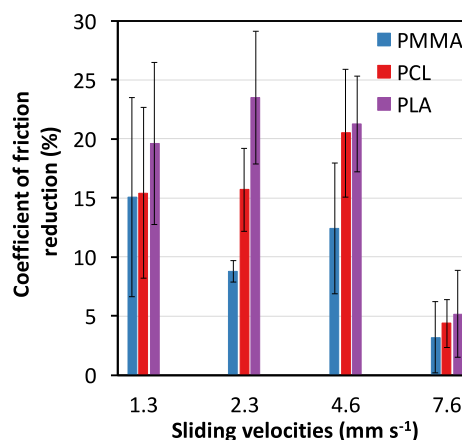
Fig. 7. Reduction of the coefficient of friction caused by PMMA, PCL, and PLA NPs formulations against sliding velocity between a steel ball and a SE substrate. Formulations consisted of NPs (0.5%), HA (0.1%), and SDS (0.5%) in PBS. The error bars represent standard error from five repetitions of the same sample.

vary.

The frictional behaviour of the formulations on the Steel-SE configuration fitted well (R^2: 0.90–0.96) by the random forest algorithm, of which the R^2 and the CC$_{cof\text{-}vel}$ for each formulation are presented in Table 4. The negative CC$_{cof\text{-}vel}$ values represent the slope of the curves and denote the negative correlation of the CoF with the sliding velocity. The more negative the CC$_{cof\text{-}vel}$, the steeper the decrease of CoF. As such, PBS demonstrated the steepest decrease in CoF, followed by PLA, PMMA, and PCL formulations. The CoF in the PCL formulation was almost stable with the sliding velocity, as confirmed by the weak CC$_{cof\text{-}vel}$.

Fig. 7 presents the averaged reduction in CoF provided by the different NPs formulations, of which the reduction rate is shown for four selected sliding velocities (up to 8 mm s^{-1}). The CoF reduction rate decreases with an increasing sliding velocity for all formulations probably because the contact was transitioning from mixed to elastohydrodynamic regime. The observation highlights the effectiveness of the

Table 4
Fitting of the tribological performance of the PMMA, PCL, and PLA nanoparticle formulations with the random forest algorithm.

Formulation	R^2 (−)	CC$_{cof\text{-}vel}$ 10^{-2} (−)
PBS	0.96	−1.5
PMMA	0.90	−0.7
PCL	0.90	−0.6
PLA	0.95	−0.8

developed formulation to reduce the CoF at the beginning of joint movement (low sliding speed). The averaged reduction was $10.7 \pm 1.4\%$ for PMMA, $14.2 \pm 1.6\%$ for PCL, and $15.2 \pm 2.1\%$ for PLA. We show that the PLA NPs based formulation was the most effective one, especially at low sliding velocity, providing a maximum reduction of 24.29%. In addition, the PLA NPs based formulation provided the lowest CoF compared to the other formulations for the entire range of sliding velocities surveyed (Fig. 6).

Although all NP based formulations show a tribological characteristics of mixed lubrication regime, the absolute values of CoF produced by PLA NPs were smaller than those by PMMA and PCL. The excellent lubrication offered by PLA based formulation might be attributed to its low viscosity, in comparing to PBS buffer and the other two solutions (Fig. 2). The other possible consideration is that PLA nanoparticles were able to remain dispersed in the full formulation, unlike PCL NPs (Fig. 1) that were notably greater in terms of hydrodynamic diameter, which resulted in a less satisfactory lubrication profile. Lastly, we speculate that the hardness of nanoparticles could play a role, e.g. hardness of PLA is 21% lower than PMMA (Table 1), implying that soft and deformable nanoparticles might be preferable to the hard ones. This requires further investigation whereby Young's modulus of the NPs is varied.

4. Summary

In the present work, a series of NP formulations, polymer NPs, HA, and SDS dispersed in PBS, were developed as prototype for IAI treatment of early stage osteoarthritic joints. Attempts were made to optimise the formulation composition in accomplishing desirable tribological and rheological profiles that meet the application condition, and to ensure long term stability for future scaling up.

Our results evidence that the NP formulations can effectively reduce the CoF under conditions that replicate the sliding of the joints at the beginning of their movement (low sliding velocities). To this end, the well dispersed NPs proved to be excellent lubricant additives, which is likely due to their adsorption on rough surfaces, rending the surface to become smooth and reduce friction. Making sure that NPs present at the contact interface could a critical design parameter for future IAI formulation based on NPs. Hyaluronic acid, a compound used in conventional IAI formulation, was shown to modulate the rheological profile of synovial fluid, in a synergistic fashion alongside NPs, and SDS enhanced the stability of the formulation. All three polymeric NPs proved capable of reducing the CoF. However, PLA based NPs provided the highest CoF reduction rate, suggesting that the mechanical properties of nanoparticles could have a considerable impact on the macroscopic tribological characteristics of the synovial joint. Naturally, biological aspects of the NPs, such as biocompatibility, inflammatory reactions, and toxicity, need to be considered in the next step of the development, alongside drug release profile. Another consideration for future work is to evaluate the effect of measurement configuration, e.g. multi-directional sliding, rolling, on the lubrication enhancement of polymeric NPs.

Declaration of Competing Interest

The authors declare that they have no known competing financial interests or personal relationships that could have appeared to influence the work reported in this paper.

Data availability

Data will be made available on request.

Acknowledgments

References

[1] S. Knecht, B. Vanwanseele, E. Stüssi, A review on the mechanical quality of articular cartilage – implications for the diagnosis of osteoarthritis, Clin. Biomech. 21 (10) (2006) 999–1012.

[2] D. Chen, et al., Osteoarthritis: toward a comprehensive understanding of pathological mechanism, Bone Res. 5 (2017) 16044.

[3] P. Wehling, et al., Effectiveness of intra-articular therapies in osteoarthritis: a literature review, Ther. Adv. Musculoskeletal Dis. 9 (8) (2017) 183–196.

[4] N. Gerwin, C. Hops, A. Lucke, Intraarticular drug delivery in osteoarthritis, Adv. Drug Deliv. Rev. 58 (2) (2006) 226–242.

[5] F. Silverstein, et al., Gastrointestinal toxicity with celecoxib vs nonsteroidal anti-inflammatory drugs for osteoarthritis and rheumatoid arthritis: the class study: a randomized controlled trial, Jama 284 (10) (2000) 1247–1255.

[6] L. Guenther, et al., Biochemical analyses of human osteoarthritic and periprosthetic synovial fluid, Proc. Inst. Mech. Eng., Part H 228 (2) (2014) 127–139.

[7] F. Russo, et al., Platelet rich plasma and hyaluronic acid blend for the treatment of osteoarthritis: rheological and biological evaluation, PLoS One 11 (6) (2016).

[8] M. Morgen, et al., Nanoparticles for improved local retention after intra-articular injection into the knee joint, Pharm. Res. 30 (1) (2013) 257–268.

[9] K. Schulze, et al., Intraarticular application of superparamagnetic nanoparticles and their uptake by synovial membrane—an experimental study in sheep, J. Magn. Magn. Mater. 293 (1) (2005) 419–432.

[10] S. Chan, et al., Atomic force microscope investigation of the boundary-lubricant layer in articular cartilage, Osteoarthr. Cartil. 18 (7) (2010) 956–963.

[11] S. Lee, et al., Frictional response of normal and osteoarthritic articular cartilage in human femoral head, Proc. Inst. Mech. Eng., Part H 227 (2) (2012) 129–137.

[12] V. Adibnia, et al., Bioinspired polymers for lubrication and wear resistance, Prog. Polym. Sci. 110 (2020), 101298.

[13] H. Chen, et al., Cartilage matrix-inspired biomimetic superlubricated nanospheres for treatment of osteoarthritis, Biomaterials 242 (2020), 119931.

[14] X. Tan, et al., Mechanised lubricating silica nanoparticles for on-command cargo release on simulated surfaces of joint cavities, Chem. Commun. 55 (18) (2019) 2593–2596.

[15] G. Liu, et al., Charged polymer brushes-grafted hollow silica nanoparticles as a novel promising material for simultaneous joint lubrication and treatment, J. Phys. Chem. B 118 (18) (2014) 4920–4931.

[16] Y. Yan, et al., Euryale ferox seed-inspired superlubricated nanoparticles for treatment of osteoarthritis, Adv. Funct. Mater. 29 (4) (2019) 1807559.

[17] H. Liu, et al., Cartilage mimics adaptive lubrication, ACS Appl. Mater. Interfaces 12 (45) (2020) 51114–51121.

[18] H. Feng, et al., Polystyrene nanospheres modified with a hydrophilic polymer brush through subsurface-initiated atom transfer radical polymerization as biolubricating additive, Macromol. Mater. Eng. 305 (6) (2020) 2000135.

[19] S. Jahn, J. Klein, Hydration lubrication: the macromolecular domain, Macromolecules 48 (15) (2015) 5059–5075.

[20] Q. Zhang, et al., Neutrophil membrane-coated nanoparticles inhibit synovial inflammation and alleviate joint damage in inflammatory arthritis, Nat. Nanotechnol. 13 (12) (2018) 1182–1190.

[21] C. Kang, et al., Acid-activatable polymeric curcumin nanoparticles as therapeutic agents for osteoarthritis, Nanomedicine (N. Y., NY, U. S.) 23 (2020) 102104.

[22] R. Liggins, et al., Intra-articular treatment of arthritis with microsphere formulations of paclitaxel: biocompatibility and efficacy determinations in rabbits, Inflamm. Res. 53 (8) (2004) 363–372.

[23] A. Bettencourt, A. Almeida, Poly(methyl methacrylate) particulate carriers in drug delivery, J. Microencapsul. 29 (4) (2012) 353–367.

[24] Food_and_Drug_Administration, Class II Special Controls Guidance Document: Polymethylmethacrylate (PMMA) Bone Cement - Guidance for Industry and FDA 668, Food and Drug Administration, U.S.A, 2002. F.A.D. Administration, Editor.

[25] B. Tyler, et al., Polylactic acid (PLA) controlled delivery carriers for biomedical applications, Adv. Drug Deliv. Rev. 107 (2016) 163–175.

[26] E. Malikmammadov, et al., PCL and PCL-based materials in biomedical applications, J. Biomater. Sci. Polym. Ed. 29 (7–9) (2018) 863–893.

[27] B. Ulery, L. Nair, C. Laurencin, Biomedical applications of biodegradable polymers, J. Polym. Sci. B Polym. Phys. 49 (12) (2011) 832–864.

[28] S. Balos, et al., Modulus of elasticity, flexural strength and biocompatibility of poly (methyl methacrylate) resins with low addition of nanosilica, Res. & Rev.: J. Dent. Sci. 4 (1) (2016) 26–33.

[29] S. Park, M. Chao, P. Raj, Mechanical properties of surface-charged poly (methyl methacrylate) as denture resins, Int. J. Dent. 2009 (2009).

[30] S. Tröster, J. Kreuter, Influence of the surface properties of low contact angle surfactants on the body distribution of 14C-poly (methyl methacrylate) nanoparticles, J. Microencapsul. 9 (1) (1992) 19–28.

[31] R. Holmes, R. Burford, C. Bertram, Preparation and characterization of poly (methyl methacrylate) beads, J. Appl. Polym. Sci. 109 (3) (2008) 1814–1822.

[32] P. Spasojevic, et al., The mechanical properties of a poly (methyl methacrylate) denture base material modified with dimethyl itaconate and di-n-butyl itaconate, Int. J. Polym. Sci. 2015 (2015).

[33] M. Dziadek, et al., New generation poly (ε-caprolactone)/gel-derived bioactive glass composites for bone tissue engineering: part I. Material properties, Mater. Sci. Eng. C 56 (2015) 9–21.

[34] B. Chen, K. Sun, Poly (ε-caprolactone)/hydroxyapatite composites: effects of particle size, molecular weight distribution and irradiation on interfacial interaction and properties, Polym. Test. 24 (1) (2005) 64–70.

[35] E. Tamjid, et al., Effect of particle size on the in vitro bioactivity, hydrophilicity and mechanical properties of bioactive glass-reinforced polycaprolactone composites, Mater. Sci. Eng. C 31 (7) (2011) 1526–1533.

[36] G. Salmoria, et al., The effects of laser energy density and particle size in the selective laser sintering of polycaprolactone/progesterone specimens: morphology and drug release, Int. J. Adv. Manuf. Technol. 66 (5–8) (2013) 1113–1118.

[37] E. Rudnik, Compostable Polymer Materials, Elsevier, 2010.

[38] T. Kasuga, et al., Preparation and mechanical properties of polylactic acid composites containing hydroxyapatite fibers, Biomaterials 22 (1) (2000) 19–23.

[39] A. Mathew, K. Oksman, M. Sain, Mechanical properties of biodegradable composites from poly lactic acid (PLA) and microcrystalline cellulose (MCC), J. Appl. Polym. Sci. 97 (5) (2005) 2014–2025.

[40] P. Ouyang, et al., Fabrication of hydrophilic paclitaxel-loaded pla-peg-pla microparticles via seds process, Front Mater Sci China 3 (1) (2009) 15–24.

[41] S. Farah, D. Anderson, R. Langer, Physical and mechanical properties of pla, and their functions in widespread applications—a comprehensive review, Adv. Drug Deliv. Rev. 107 (2016) 367–392.

[42] J. Ferri, et al., Poly (lactic acid) formulations with improved toughness by physical blending with thermoplastic starch, J. Appl. Polym. Sci. 135 (4) (2018) 45751.

[43] J. Dunkers, M. Cicerone, N. Washburn, Collinear optical coherence and confocal fluorescence microscopies for tissue engineering, Opt. Express 11 (23) (2003) 3074–3079.

[44] C. Goncalves, J. Coutinho, I. Marrucho, Optical properties, in: R. Auras, et al. (Eds.), Poly(Lactic Acid): Synthesis, Structures, Properties, Processing, and Applications, 2010.

[45] H. Butt, B. Cappella, M. Kappl, Force measurements with the atomic force microscope: technique, interpretation and applications, Surf. Sci. Rep. 59 (1–6) (2005) 1–152.

[46] V. Juras, et al., In vitro determination of biomechanical properties of human articular cartilage in osteoarthritis using multi-parametric MRI, J. Magn. Reson. 197 (1) (2009) 40–47.

[47] A. Vidal-Lesso, et al., Mechanical characterization of femoral cartilage under unicompartimental osteoarthritis, Ingeniería Mecánica, Tecnología y Desarrollo 4 (6) (2014) 239–246.

[48] M. Stolz, et al., Dynamic elastic modulus of porcine articular cartilage determined at two different levels of tissue organization by indentation-type atomic force microscopy, Biophys. J. 86 (5) (2004) 3269–3283.

[49] A. Thambyah, A. Nather, J. Goh, Mechanical properties of articular cartilage covered by the meniscus, Osteoarthr. Cartil. 14 (6) (2006) 580–588.

[50] S. Ghosh, et al., Investigation of techniques for the measurement of articular cartilage surface roughness, Micron 44 (2013) 179–184.

[51] A. Peters, et al., The effect of ageing and osteoarthritis on the mechanical properties of cartilage and bone in the human knee joint, Sci. Rep. 8 (1) (2018) 1–13.

[52] M. Gardner-Morse, et al., In situ microindentation for determining local subchondral bone compressive modulus, J. Biomech. Eng. 132 (9) (2010).

[53] T. Mills, Development of in-vitro mouth methods for studying oral phenomena, in: School of Chemical Engineering, University of Birmingham, Birmingham, Uk, 2011.

[54] J. de Vicente, J. Stokes, H. Spikes, Soft lubrication of model hydrocolloids, Food Hydrocoll. 20 (4) (2006) 483–491.

[55] Z. Zhang, D. Simionesie, C. Schaschke, Graphite and hybrid nanomaterials as lubricant additives, Lubricants 2 (2) (2014) 44–65.

[56] M. Temple-Wong, et al., Hyaluronan concentration and size distribution in human knee synovial fluid: variations with age and cartilage degeneration, Arthritis Res. Ther. 18 (2016) 18.

[57] X. Ye, et al., Depletion interactions in colloid-polymer mixtures, Phys. Rev. E 54 (6) (1996) 6500.

[58] G. Georgiev, et al., Surface chemistry study of the interactions of hyaluronic acid and benzalkonium chloride with meibomian and corneal cell lipids, Soft Matter 9 (45) (2013) 10841–10856.

[59] M. Rosen, J. Kunjappu, Surfactants and Interfacial Phenomena, John Wiley & Sons, 2012.

[60] H. Barnes, A Handbook of Elementary Rheology vol. 1, University of Wales, Institute of Non-Newtonian Fluid Mechanics Aberystwyth, 2000.

[61] M. Pancharoen, Physical properties of associative polymer solutions, in: Energy Resources Engineering, Stanford University, California, USA, 2009.

[62] J. De Vicente, J. Stokes, H. Spikes, Lubrication properties of non-adsorbing polymer solutions in soft elastohydrodynamic (EHD) contacts, Tribol. Int. 38 (5) (2005) 515–526.

[63] V. Rudyak, Viscosity of nanofluids. Why it is not described by the classical theories, Adv. Nanopart. 2 (03) (2013) 266.

[64] H. Chen, Y. Ding, C. Tan, Rheological behaviour of nanofluids, New J. Phys. 9 (10) (2007) 367.

[65] J. Necas, et al., Hyaluronic acid (hyaluronan): a review, Vet. Med. 53 (8) (2008) 397–411.

[66] S. Haward, et al., Extensional flow of hyaluronic acid solutions in an optimized microfluidic cross-slot device, Biomicrofluidics 7 (4) (2013).

[67] S. Thomas, C. Sobhan, A review of experimental investigations on thermal phenomena in nanofluids, Nanoscale Res. Lett. 6 (1) (2011) 377.

[68] P. Mishra, et al., A brief review on viscosity of nanofluids, Int. Nano Lett. 4 (4) (2014) 109–120.

[69] T. Yalçın, et al., The viscosity and zeta potential of bentonite dispersions in presence of anionic surfactants, Mater. Lett. 57 (2) (2002) 420–424.

[70] M. Gulzar, et al., Tribological performance of nanoparticles as lubricating oil additives, J. Nanopart. Res. 18 (8) (2016) 1–25.

[71] Y. Shimizu, H. Spikes, The influence of slide–roll ratio on zddp tribofilm formation, Tribol. Lett. 64 (2) (2016) 19.